Environmental Science
Water Research & Technology

ROYAL SOCIETY OF CHEMISTRY

PAPER

View Article Online
View Journal | View Issue

Cite this: *Environ. Sci.: Water Res. Technol.*, 2025, **11**, 714

Behaviour of particle mobilization and reattachment under flushing conditions in PVC pipes using a full-scale laboratory system

Benjamin Anderson, Artur Sass Braga,* Yves Filion and Sarah Jane Payne

Excessive accumulation of particulate material and biofilms on the inner walls of drinking water pipes increases the risk of water discoloration events, known to be the major cause of customer complaints worldwide. As a result, water utilities use pipe flushing operations to mobilize material deposits from 'dirty sections' of their pipe networks. Nevertheless, the development of preventative strategies is still limited by the lack of knowledge about the material accumulation process and the behaviour of resuspended particles during flushing. The goal of this paper is to investigate the behaviour of insoluble iron oxide particles during controlled accumulation and flushing processes in PVC drinking water pipes. A set of four experiments was completed where water with a known concentration of iron oxide particles was introduced into a full-scale pipe loop laboratory system under steady flow conditions producing the accumulation of particles along half the pipe length. The system was then flushed using two sequential velocities (0.7 and 1.2 m s^{-1}) and the direction of flush was changed between each independent flushing stage. During the flushing operations, it was found that a small number of mobilized particles can reattach to downstream sections pipes, and resist mobilization to elevated wall shear stresses of 1.2 Pa. Furthermore, even after successive flushes in one direction, a subsequent flush of equal velocity in the opposite direction was able to mobilize new particles from the pipe wall surface. These findings revealed a new mechanism of particle resistance to mobilization that is independent of the WSS. These results may assist water utilities in improving flushing strategies for DWDSs and managing accumulated material in their networks.

Received 17th September 2024,
Accepted 10th January 2025

DOI: 10.1039/d4ew00764f

rsc.li/es-water

Water impact

This paper investigates the behavior of particulate material during flushing operations in a full-scale laboratory drinking water distribution system. Resuspended particles were found to reattach to pipes during flushing, and their resistance to mobilization was also impacted by the flow direction. Results aim to assist water utilities to improve flushing strategies and manage particle accumulation in their systems.

1.0 Introduction

The accumulation and mobilization of sediment and biofilms in drinking water distribution systems (DWDSs) are caused by several factors that include high flow events, pipe breaks, and pump trips. For example, in the case of a fire, first responders typically draw water from the DWDS at a high flow rate through a hydrant connection. This in turn increases the fluid velocities and wall shear stresses (WSSs) in the local distribution pipes and can cause material mobilization.[1] The WSS is a tangential force produced by water flow over the pipe wall that pulls materials adhered to the pipe wall surface into the flow direction. Its average magnitude is dependent on the fluid velocity and absolute roughness of the pipe, and can be calculated using the Darcy–Weisbach equation (eqn (1)):

$$\tau = \frac{1}{8} f_D \rho V^2 \quad (1)$$

where τ is the WSS (Pa); f_D is the Darcy–Weisbach friction factor; ρ is the water density (kg m^{-3}); and V is the average fluid velocity in the pipe (m s^{-1}).

The material shear strength (MSS) in contrast is a measure of the adhesion and cohesion forces of accumulated material on pipe walls. When WSS exceeds MSS, the mobilization of accumulated material occurs.[2,3] Material released during discolouration events is often of differing size and density and it can originate from processes within the DWDS such as corrosion, salt and metal precipitation, and biofouling.[4]

Department of Civil Engineering, Queen's University, Kingston, Ontario, Canada. E-mail: 16asb2@queensu.ca; Tel: +1 (613) 483 4511

Discolouration events tend to be dominated by metals such as iron and manganese.[5] Although iron and manganese often cause aesthetic issues,[6,7] manganese has been associated with harmful neurological impacts,[8,9] and drinking water regulations and guidelines have reflected the need to manage manganese from a health perspective.[10,11] Because discolouration is highly visible to consumers, it is the leading cause of complaint among customers to their water utility companies.[6] The obligation to meet new regulations and address customer complaints means that discolouration events can also have financial implications for water utility companies. These factors have spurred water utilities to develop techniques to reduce the buildup of material deposits within DWDSs.

Currently, pipe flushing is one of the most powerful tools that water utilities use to address issues with material accumulation in DWDSs. Conventional flushing consists of opening hydrants in specific areas of a DWDS until preselected water quality targets are achieved. These targets could include detectable disinfectant residual, reduction/elimination of discoloured water, and a reduction in turbidity. Since valves are not closed to isolate segments of pipes in conventional flushing, water flows from multiple mains to the hydrant and this seldom maximizes fluid velocities.[12,13] This lowers the cleaning efficiency of the procedure. Despite this, conventional flushing remains popular because it is effective at restoring disinfectant residuals by refreshing old water in the pipes, and being easy to perform compared to other flushing techniques.[12,13]

Alternatively, unidirectional flushing (UDF) is a technique originally proposed by Oberoi[14] that has gained popularity among water utilities and discolouration research.[1–3,5,15] UDF involves isolating a pipe section or loop through valve closures to flush a pipe segment in a single direction.[16] The fluid velocities used in UDF must provide sufficient scouring action on the surface of the distribution pipes to remove sediments, biofilms, and loose deposits. The velocity most associated with UDF is approximately 1–2 m s^{-1} within each pipe segment.[16] An ideal UDF procedure calls for a sequential deployment that begins at the treatment plant or source and progresses to the periphery of the DWDS with flushed water expelled from the system. In practice this is seldom accomplished due to the resources required to flush an entire DWDS and some water utilities have chosen to flush a select number of neighbourhoods (3–10) per year.[12] Specific factors such as fluid velocity and flush duration needed to effectively clean distribution pipes have proven to be site specific and dependent on accumulation period, treated water characteristics, and pipe material.[5,13] Although UDF is recognized to be an effective method of maintaining water quality in DWDSs, UDF operations are considered expensive, use large amounts of water, and require the isolation of pipe sections which can lead to temporary discontinuance of service to consumers. These shortcomings have encouraged researchers to better understand pipe wall material dynamics in DWDSs and utilize network simulation to design more efficient and effective cleaning protocols.[4,6,17]

Despite noticeable short-term improvements after flushing, the positive effects on water quality have been shown to be short lived. Research has shown that the benefits of traditional flushing may only last for approximately 14 days after flushing and the accumulated material loads were similar only one year after flushing.[18] The complicated behaviour of material mobilization due to flushing in DWDSs leaves many unanswered questions regarding the effectiveness of flushing to improve long-term water quality. Clearly, flushing protocols induce the mobilization of loose and built-up material from the internal surface of pipes, but the fate of the mobilized material and how it behaves in suspension is not well understood. These questions motivate the need for the present controlled lab experiment to monitor particles before, during, and after flushing protocols in a full-scale pipe system. It is theorized that, even under flushing flow conditions, the reattachment of mobilized particles occurs more quickly and at higher rates than previously understood.[19]

A key and potentially overlooked aspect of UDF application is the direction of flushing flow. It has been suggested that the spatial arrangement of iron particles on the wall of PVC pipes devoid of any biofilm depends in part on the conditioning flow field in the pipe, and the size of the particles moving through the pipe relative to the roughness elements of the pipe to which they eventually become adhered.[20] Along these lines, whether a particle will be mobilized by higher flows and WSS when a pipe is flushed depends in part on how well a roughness "valley" can protect the particle that is seated in it against the WSS induced by the flow in the pipe. Furthermore, areas such as the inner radius of curved sections can create water recirculation zones with low WSS where material can easily accumulate. Switching the flushing direction can shift the location of recirculation zones, exposing the accumulated material to higher WSS. Additionally, DWDS features such as dead ends and pipe fittings can create dead zones in a network where particles can accumulate and become protected from one flow direction. Material accumulated in these dead zones could be susceptible to mobilization if the flushing direction is changed. These factors suggest that flushing in the opposite direction to the operational flow of a DWDS may mobilize material that was otherwise protected in the operational direction.

In this context, this paper aims to examine the behaviour of particle mobilization and reattachment in PVC pipes during controlled flushing experiments after the deposition of iron oxide *via* the circulation of a concentrated particle plug in a full-scale PVC pipe loop system. Specifically, the objectives of the experiments were to (1) investigate the behaviour of iron oxide deposition using a particle plug and the total mass of iron oxide deposited on certain sections of the PVC pipe loop; (2) investigate the dynamics of particle mobilization during flushing using a reverse flow direction;

and (3) determine the extent to which direction alone is a factor at mobilizing seated particles from the surface of PVC pipes.

2.0 Materials and methods

The experimental program was performed in the Drinking Water Distribution Laboratory (DWDL) at Queen's University – a unique research facility capable of partially replicating hydraulic conditions of operational DWDSs. A full-scale pipe loop system with 193 m of 108 mm internal diameter IPEX Blue Brute pipes was used for the experiments in an open-end configuration (Fig. 1): (i) local drinking water is supplied to a 3800 L tank, (ii) centrifugal pumps draw water from the tank and pump it into the pipe-loop entrance, and (iii) after flowing through the pipes, the water is discarded into a drain. The entire pipe loop system is in a temperature-controlled chamber with online sensors that monitor the tank level, pipe flow rate, pressure, temperature, and turbidity. Fig. 1 shows the pipe loop system with the longitudinal locations of the turbidimeters, sample ports, and the injection point (discussed below) in both plan and profile views.

A set of four experiments (A, B, C, and D) were performed, each divided into two phases: loading and flushing. Experiments A and B are classified as high loading flow experiments while experiments C and D are low loading flow experiments (Table 1). In the experiments, inert and insoluble synthetic ferric oxide (Fe_2O_3) were injected into the middle of the pipe loop to promote their accumulation on only the second half of the pipe loop length. These particles are commonly produced from corrosion of cast iron pipes,[21] and were selected for focus the experiment investigation on the impact of system hydrodynamics on particulate material.[3] Precise control over particle injection was achieved using a diaphragm pump that drew water from a large mixing tank with a known particle concentration. This setup allowed the production of finite 'particle plugs' traveling through the pipe-loop, which were designed to a length of 240 m and concentration of 20 mg L^{-1}. The loading phase of each experiment consisted of the passage of a total of two particle plugs to allow a higher quantity of particles to be deposited at the pipe wall. After the exit of the particle plugs from the pipe loop the steady flow was maintained until an additional volume of 1.5 pipe loops was passed through the system.

Following the loading phase in each experiment, the pipe-loop was flushed using a sequence of four flushing stages (F1–F4) in different combinations of flow directions and flow rates to examine the effectiveness of changing the flow direction in mobilizing material from the pipe wall. F1 and F2 were executed at a velocity of 0.7 m s^{-1}, while F3 and F4 were performed at a flow rate of 1.2 m s^{-1}. Table 1 shows the hydraulic parameters during all stages of the experiments. The flushing sequence of experiments A and C started with a forward flush step (FFS1), which was then alternated to a reverse flush step (RFS1), and then this sequence of direction was repeated at a higher flushing magnitude (FFS2 and RFS2). Meanwhile, the flushing sequence of experiments B and D was inverted, starting with RFS1, followed by FFS1, RFS2 and FFS2. Fig. 2 illustrates the flushing sequence for all 4 experiments. In each flushing step, a total of three pipe-loop volumes were used to flush the pipes, followed by an additional two repetitions of the full flushing step with the exact same conditions. This guaranteed that all mobilized material was flushed out the system before the next step.

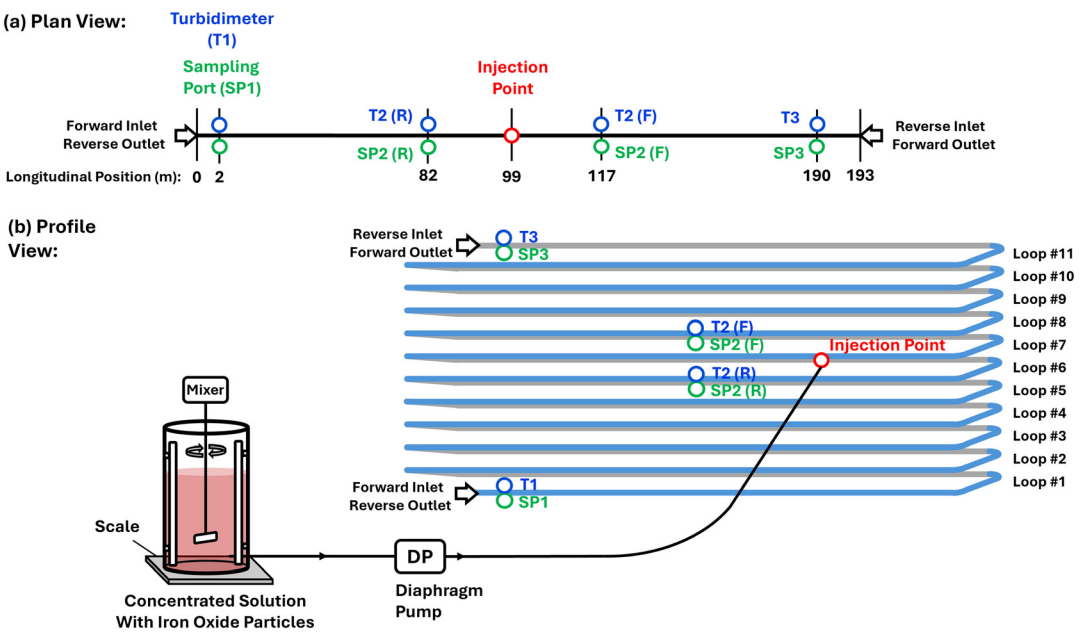

Fig. 1 (a) Plan view schematic of the pipe loop with the location of turbidimeters, sample ports, and injection point. (b) Profile view schematic of the pipe loop with the locations of turbidimeters, sample ports, injection point, tank mixer, and diaphragm pump.

Table 1 Hydraulic parameters of the PVC pipe loop for the different stages of the experiments

Experiment stage	Flow rate (L s^{-1})	Velocity (m s^{-1})	Wall shear stress (Pa)	Reynolds number	Total duration (minutes)
Loading phase, high loading flow experiments (A, B)	0.90	0.10	0.04	10 600	210
Loading phase, low loading flow experiments (C, D)	0.60	0.07	0.02	7000	300
Flushing phase, flushing steps F1 and F2	6.50	0.70	1.20	76 600	42
Flushing phase, flushing steps F3 and F4	11.0	1.20	3.09	13 000	24

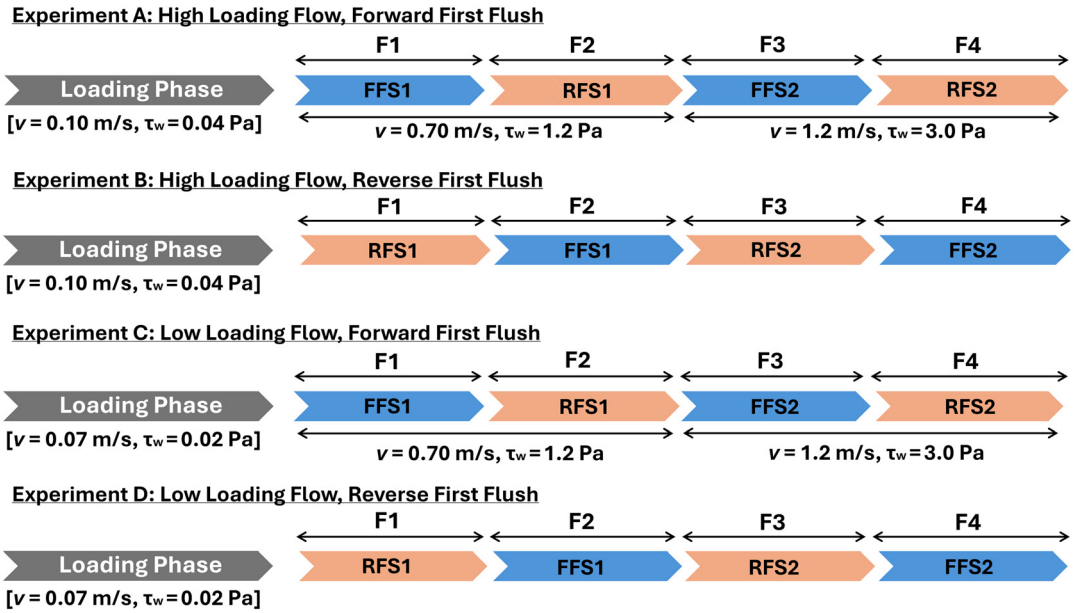

Fig. 2 Description and order of stages for experiments A, B, C, and D.

Continuous high-resolution turbidity measurements (1 Hz) were collected with three Hach TU5300sc turbidimeters T1, T2, and T3, located at the entrance, middle, and exit of the pipe-loop. Here, T2 is located 18 m from the injection point which means that it is 20% of the distance between the injection point and the exit of the pipe loop at T3 of 91 m. The filtered drinking water used to refresh the system had a baseline turbidity of 0.040 NTU. In addition, several bulk water samples were collected throughout the experiments to assess the suspended sediment concentration (SSC) and particle size distribution (PSD).

Bulk water samples were taken from the centerline of the pipes at three sample ports SP1, SP2, and SP3 at locations mirroring the turbidimeters at the entrance, middle, and exit of the pipe-loop as indicated in Fig. 1. The SSC was measured through a traditional gravimetric method using glass-fiber filter membranes with a pore size of 0.7 μm.

The particle size distribution (PSD) of bulk water samples was analyzed using a Malvern Mastersizer 3000 which uses laser diffraction to measure particle size distributions from 10 nm to 3.5 mm. Refined turbidity data and SSC measurements were combined to determine the mass of iron oxide particles deposited and mobilized during all phases of the experiments using the method developed by Braga and Filion.[20] Distinct calibration coefficients were calculated based on the real time turbidity data corresponding to the SSC samples. The four experiments were separated into two groups, the high loading flow and low loading flow experiments, based on the loading phase hydraulic conditions. Separate coefficients were created to represent the SSC samples taken from sample port 2 (SP2) and sample port 3 (SP3). A total of four coefficients were used in the loading phase analysis. In comparison, only one coefficient was calculated for all the flushing phases due to the higher variability of PSD and concentration. In this case, SSC and turbidity measurements were taken from the furthest downstream sampling point for each flushing step. The concentration of each SSC sample was combined with the average turbidity over the duration of the sample. The result yielded the coefficient as a concentration in relation to turbidity as shown in eqn (2):

$$\mathrm{SSC\ (mg\ L^{-1})/Turb_{avg}\ (NTU)} = \alpha\ \mathrm{(mg\ L^{-1}\ NTU^{-1})} \quad (2)$$

By combining the coefficients with the real-time flow and turbidity data, a mass flux (M_f) of suspended particulate material was estimated using eqn (3):

$$M_f\ \mathrm{(mg\ s^{-1})} = \alpha\ \mathrm{(mg\ L^{-1}\ NTU^{-1})} \times \mathrm{Turb\ (NTU)} \times Q\ \mathrm{(L\ s^{-1})} \quad (3)$$

The integration of the mass flux curves, as shown in eqn (4), yielded mass values at each phase of the experiment (M_T) that were used to interpret the quantity of material added to the system during the loading phase and the amount removed during flushing. The material removed from flushing for each experiment was analysed and the results of the forward and reverse tests were compared to see the role that direction plays in mobilizing iron oxide particles from the pipe wall surface.

$$M_T = \int_T M_f dt \quad (4)$$

here, t = time (seconds) and T = period over which suspended materials are deposited or mobilized from the pipe wall (seconds).

The mass of particles injected into the pipe loop was calculated by using SSC samples from the mixing tank and the measured volume of the concentrated particle water mixture pumped into the pipe loop for each experiment. The differences between the calculated mass injected into the system and the calculated mass that passed through T2 and T3 were used to determine the mass of material deposited between the injection point and T2, and the mass of material deposited between T2 and T3.

3.0 Results

The first objective of this paper was to investigate the behaviour of iron oxide deposition using a particle plug and determine the total mass of iron oxide deposited on certain sections of the PVC pipe loop. The real-time turbidity data and the corresponding SSC samples taken for each particle plug were analyzed from the loading phase. The results of the iron oxide particle deposition during the loading phase are summarized in Table 2. Overall, an average of 70% of the total material mass injected into the loop was deposited along the pipes of the loop across all experiments during the loading phase; the remaining material exited the pipe loop. An average of 62% of the total material deposited in the pipes was accumulated in the first 20% of the pipe loop length (between the injection point and T2), indicating a faster deposition rate of particles right after their injection in the system.[22]

The second objective was to investigate the dynamics of particle mobilization during flushing using a reversed flow direction. Mass flux curves were examined for the respective flushing phases of each experiment and used to characterize particle behaviour. Fig. 3 shows the mass flux profiles of flushing stage 1 (F1) for all experiments. Curves in Fig. 3 showed a rise to a peak mass flux followed by a decline that indicates the arrival of the freshwater front at the exit of the pipe loop. A more gradual increase and a sharper decrease in mass flux were observed for the forward first stage experiments (experiments A and C in Fig. 3) with peaks at approximately 0.5 pipe loop turnovers. A pipe loop volume turnover describes the portion of the total pipe loop volume (not including the tank reservoir) that has passed through the outlet of the system. Therefore 0.5 pipe loop turnovers correspond to the water located in the center of the pipe loop near the injection point. A sharper increase in mass flux and more gradual decrease was observed in the reverse first stage experiments (experiments B and D in Fig. 3), including a small increase around 1.0 pipe loop volume turnovers. The low loading flow experiments showed higher peaks in mass flux than the high loading flow experiments; this indicates a higher rate of particle deposition in the low loading flow experiments. However, the similarities in the shape of the turbidity curves between forward first stage and reverse first stage experiments show that the behavior of particle mobilization was consistent across experiments with the same flushing order. Fig. 4 shows the mass flux profiles from flushing stage 2 (F2), where the pipes were flushed at the same flow rate as in F1 but in the opposite flow direction. The mass flux rate had substantially smaller magnitudes, but consistent mobilization of particles from the pipe walls was still observed. For example, when the direction is changed, the forward first stage (A and C) and reverse first stage (B and D) experiments correspond to RFS1 and FFS1 respectively. Mass flux plots in Fig. 4 show two distinct peaks in mass flux at pipe loop volume turnovers of 0.5 and 1.0. Surprisingly, the increase in mass flux in flushing stage 2 occurred earlier in experiments B and D (Fig. 4), which were flushed in the reverse direction in flushing stage 1. Meanwhile for experiments A and C (Fig. 4), the increase of mass flux rate occurred at the expected mark of 0.5 pipe loop turnovers – the same position where particles were initially

Table 2 Accumulated mass of iron oxide particles during the loading phase based on the online turbidity data transformed to SSC

Experiment	A	B	C	D
Loading phase flow rate	0.9 L s^{-1}	0.9 L s^{-1}	0.6 L s^{-1}	0.6 L s^{-1}
First flush direction	Forward	Reverse	Forward	Reverse
Mass injected from the tank into the system (g) [U]	56.6	56.6	56.5	56.5
Mass detected passing through T2 (g) [V]	35.2 (62%)[a]	34.7 (61%)	29.5 (52%)	29.7 (53%)
Mass detected passing through T3 (g) [W]	22.2 (39%)	23.4 (41%)	20.4 (36%)	20.3 (36%)
Acc. mass between the injection point and T2 (g) (18 m) [$X = U - V$]	21.4 (38%)	21.9 (39%)	27.0 (48%)	26.8 (47%)
Acc. mass between T2 and T3 (g) (73 m) [$Y = V - W$]	13.0 (23%)	11.3 (20%)	9.1 (16%)	9.3 (17%)
Total acc. mass between the injection point and T3 (g) (91 m) [$Z = X + Y$]	**34.4 (61%)**	**33.2 (59%)**	**36.1 (64%)**	**36.2 (64%)**

[a] Percentages calculated based on the mass injected into the pipe loop [U].

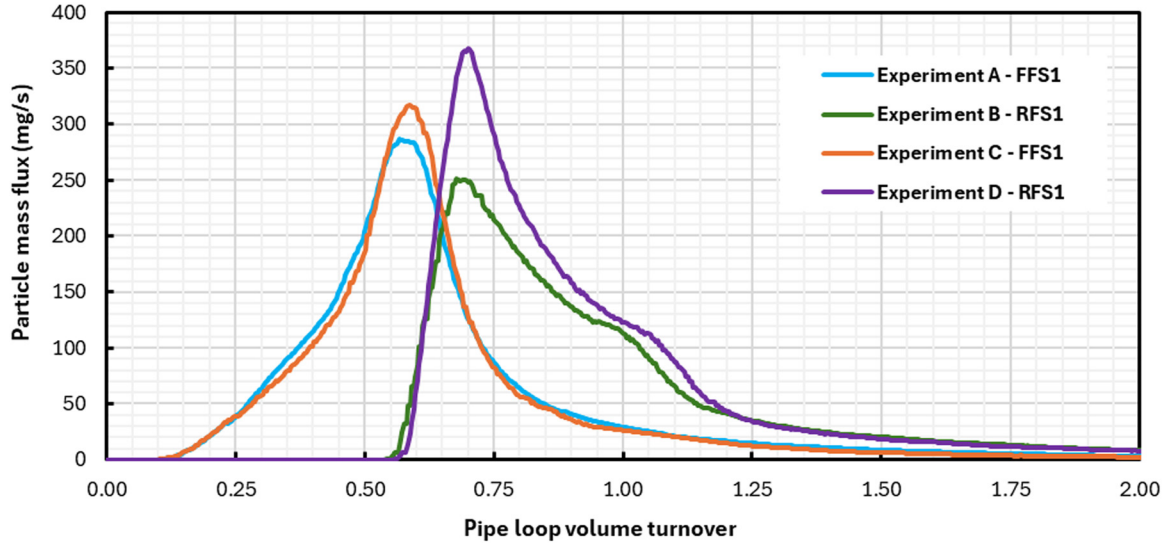

Fig. 3 Flushing stage 1 mass flux profiles measured at the outlet for exp. A – FFS1 (T3), exp. B – RFS1 (T1), exp. C – FFS1 (T3), and exp. D – RFS1 (T1).

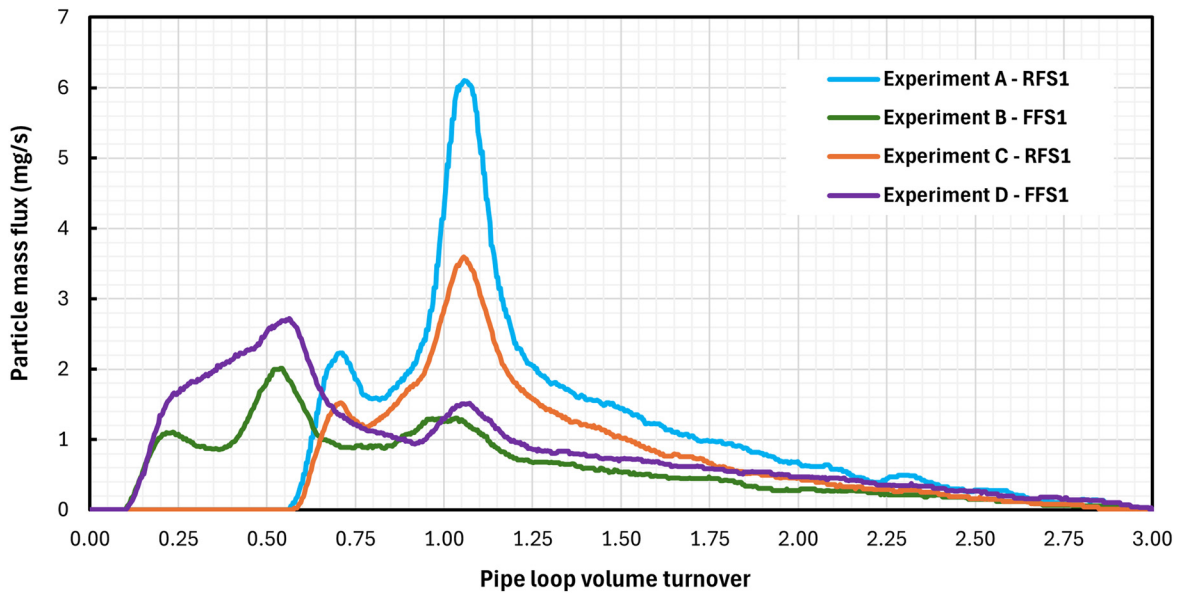

Fig. 4 Flushing stage 2 mass flux profiles measured at the outlet for exp. A – RFS1 (T1), exp. B – FFS1 (T3), exp. C – RFS1 (T1), and exp. D – FFS1 (T3).

injected in the pipe loop. These results strongly indicate that the first flushing stage in the reverse direction (experiments B and D) caused a redistribution of particles along the clean sections of the pipe loop. This also means that a fraction of the particles that were mobilized in the first flushing stage were reattached to the clean pipe sections at a high flow rate of 6.5 L s^{-1} and WSS of 1.2 Pa. This is shown in Fig. 5 where the first 50% of the pipe loop remains devoid of particles after flushing stage 1 for experiments A and C while the reverse flush in flushing stage 1 in experiments B and D caused reattachment in the first 50% of the pipe loop length. This reattached material is depicted in the first 0.5 pipe loop turnovers as shown in Fig. 4 in experiments B and D. Fig. 5 also illustrates that, after flushing stage 2, particles are mobilized and redistributed throughout the entire pipe loop once it has been flushed in both the forward and reverse directions.

The turbidity and SSC data were used to ascertain how much material was removed from the system during flushing. Table 3 presents the total mass of iron oxide particles that was mobilized during each of the 4 flushing stages. A clear trend was observed across all experiments showing that an average of 94% of the total mobilized material across all flushing stages occurred in F1 followed by averages of 2%, 4% and 1% in F2, F3, and F4, respectively. This again corresponds with the findings of Braga and

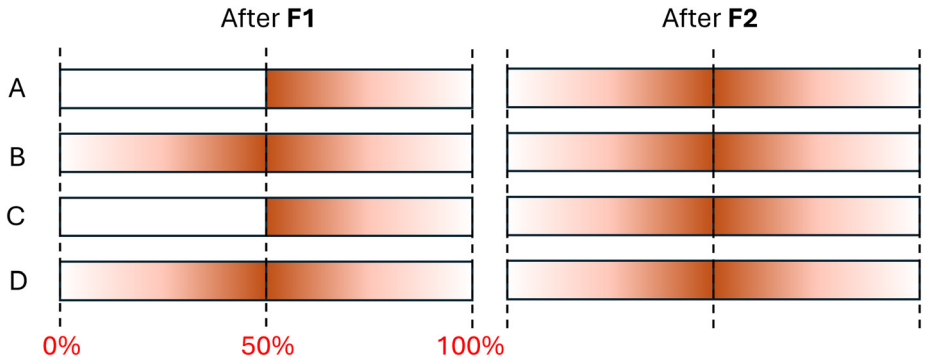

Fig. 5 Illustration of the longitudinal distribution of particles after flushing stage 1 (F1) and flushing stage 2 (F2). Dashed lines and corresponding red lettering depict the longitudinal position in terms of percentage of total pipe loop length. Here, 50% corresponds to the position of the injection point. Colour gradients represent the amount of accumulated material where the darker colour shows a higher distribution near the injection point and less towards the peripheries of the pipe loop.

Table 3 Mobilized mass of iron oxide particles during the flushing phase based on the online turbidity data transformed to SSC. Blue (shaded) cells represent a flush in the forward direction and orange (light) cells represent a flush in the reverse direction

Experiment	A	B	C	D
Loading phase flow rate	0.9 L s^{-1}	0.9 L s^{-1}	0.6 L s^{-1}	0.6 L s^{-1}
First flush direction	Forward	Reverse	Forward	Reverse
Mobilized mass for F1 (g)	28.5 (93%)[a]	28.4 (94%)	30.1 (93%)	33.5 (94%)
Mobilized mass for F2 (g)	0.8 (3%)	0.5 (2%)	0.6 (2%)	0.7 (2%)
Mobilized mass for F3 (g)	1.1 (4%)	1.0 (3%)	1.2 (4%)	1.4 (4%)
Mobilized mass for F4 (g)	0.3 (1%)	0.3 (1%)	0.4 (1%)	0.1 (0%)
Total mobilized mass (g)	**30.7**	**30.1**	**32.3**	**35.6**

[a] Percentages calculated as the mobilized mass per flushing stage per the total mobilized mass.

Filion[20] who found that the majority of accumulated iron particles were removed during the first flushing stage (F1).

After all flushing steps, the overall mobilization efficiency (percentage of mobilized material *versus* accumulated material) averaged 92%, ranging between 89 and 98% across the 4 experiments. In comparison, by considering only F1, the same metric is reduced to an average of 86%. This indicates that the combined effects of changing the flow direction and increasing the flow velocities improved the flushing efficiency by approximately 6%.

The results indicated in Table 3 also answer the third research objective, which was to assess whether there is an enhanced mobilization of particles when the flushing direction is changed. The impact of reversing the flushing direction from F1 to F2 results in an average mobilization of 2% of additional material in the pipe loop. Similarly, the impact of reversing the flushing direction from F3 to F4 results in an average mobilization of 1% of additional material in the pipe loop. Results also show that starting the flushing phase in the reverse direction (experiments B and C) did not yield a higher mobilization efficiency. This may indicate that particles mobilized in the second flushing stage in response to the reversal of flow direction could be the same particles that are able to reattach to the pipes during the first flushing stage. Meanwhile the increase of WSS in the third flushing stage triggers the mobilization of new particles.[19,23]

Lastly, Fig. 6 indicates the PSD results for different phases of the experiments, including the i) loading tank, ii) loading phase, and iii) flushing peak. In Fig. 6, the D80 of a PSD corresponds to the particle size that sums 80% of the PSD accumulated distribution. Samples collected during the loading phase showed a high variability of PSD; Fig. 6 shows their average (solid line) and their minimum and maximum values (dashed lines). In addition, during the flushing phase only the samples collected during the passage of the turbidity peak by the sample port achieved sufficient SSC to perform PSD measurements. The loading tank samples had a

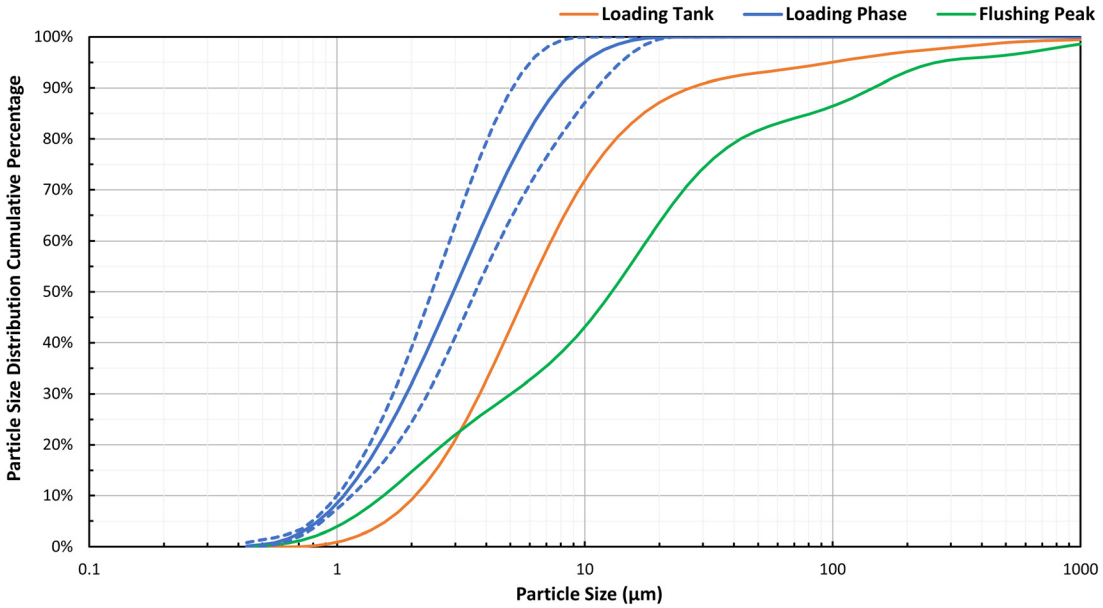

Fig. 6 Particle size distribution (PSD) of bulk water samples collected during the experiments. The primary vertical axis (left-hand side) denotes the accumulated PSD that corresponds to the particle volume which is below a corresponding particle size (horizontal axis), while D80 highlights the particle size where the cumulative curve adds to 80% of all particle volume. Loading tank samples were collected from the high concentrate solution that was injected in the pipes. Loading phase samples (solid line) is the average of multiple samples collected during the passage of the suspended particle plume in the pipes, including their minimum and maximum values (dashed lines). Flushing peak samples show the average of samples collected during the passage of the turbidity peak by the sample port.

distribution of particles ranging from 1 μm to over 100 μm with the D80 being around 15 μm.

The loading phase samples have more fine particles with little to no particles exceeding 10 μm and a D80 of 6 μm. In comparison, the samples collected during the peak of the flushing operations were composed of larger particles than that of the tank and loading phase samples, with a D80 of 40 μm. This demonstrates that the larger and heavier particles had settled on the pipes shortly after their injection in the system. This confirms the theory that iron oxide particles with sizes as small as 50 μm are able to settle in smooth PVC pipes even under turbulent flow conditions (Re = 10 610, WSS = 0.018 Pa), and are easily mobilized with flushing flow rates.[20] Furthermore, the lack of larger particles in the loading phase sample proves that larger particles have not reached SP2 and SP3 where the loading phase samples were taken, and were accumulated in the first 20% of the pipe loop length.

4.0 Discussion

During the loading phase of the experiments, the fluid velocity was found to affect the deposition rate of particles. In experiments A and B, with the higher loading velocity, 60% of particle mass injected into the loop was deposited onto the pipe wall; in experiments C and D with the lower loading velocity, 64% of particle mass injected into the loop was deposited onto the pipe wall. Despite the low number of trials realized here, it is hypothesised that extra particles are held in suspension in the higher velocity experiments, which also aligns with previous findings from similar experiments reported by Braga and Filion.[20] This suggests that increasing the fluid velocity increases the particle size threshold that divides suspended and pipe-wall-attached particles.

Particles attached to the pipe wall surface can be classified according to their resistance to mobilization – a metric that is traditionally based on the WSS that is required for mobilization, also known as material shear strength (MSS).[3] Loose particles, commonly caused by gravitational settling, have low MSS and are the first ones to be mobilized during flushing upon a small increase of the WSS. Meanwhile, particles with higher MSS and can persist even after instances of high WSS. Particles can also become conditioned by the WSS caused by the flow of water in the pipe and therefore become more adhered.[24,25] These experiments demonstrated that a large fraction of the injected particles rapidly settled to the invert of the pipes and had low MSS since they were easily mobilized by the first flushing step (F1). However, the additional mobilization detected at the second flushing step (F2) demonstrated that a particle's resistance to mobilization also has a directional dependence that was independent of the WSS, since new particles were mobilized without an increase of WSS in comparison to F1. It is hypothesised here that the 44× elbows and more than 200× smooth pipe joints of the pipe-loop may act as enhanced particle accumulation locations, where small zones of low wall shear stress are produced due to velocity profile transitions in these parts. This hypothesis is supported by the detection of particles from the whole length of the pipe loop during the flushing step F2 (Fig. 4). The enhanced

particle accumulation locations may also scale with the number of fittings and looped pipes in operational DWDSs, but further studies are required to confirm their real impact in comparison to material accumulation on straight pipe sections.

The mass flux profiles from flushing stage 1 for all experiments (Fig. 3) showed that during the passage of the particle plugs the highest loads of particles were deposited near the injection point (immediately after their injection into the pipes), but that substantial longitudinal deposition also occurred along the remainder of the pipe loop. These particle deposition patterns observed in Fig. 3 highlight how experiments C and D, with lower velocities during the loading phase, resulted in higher mass flux peaks in comparison to experiments A and B. This suggests that the settling rate of particles after injection was a function of the fluid velocity, where lower velocities promoted higher settling rates and increased the load of particles next to the injection point. This trend matches the particle deposition pattern found by Braga and Filion[19] in their experiments using the same laboratory conditions.

In the case of the second flushing stage, when the flow direction was reversed, the mass flux profiles shown in Fig. 4 highlighted a distribution of particles along the whole length of the pipes for experiments B and D, which was not observed in experiments A and C. The latter, which were previously flushed in the forward direction during the first stage, used a reverse flushing direction for the second stage and no particles were found in the first half of the pipe loop, since deposition occurred only in the second half of the loop. But for experiments B and D, which were flushed in the reverse direction in the first stage and then flushed in the forward direction during the second stage, a steady and high rate of material flux was observed at the half volume; a second peak was produced at the full-loop volume before decaying to background levels with the fresh waterfront (Fig. 4). This suggests that there was material adhered to the pipe loop section between the entrance and injection point that must have been redistributed from the reverse flush of flushing stage 1 as illustrated in Fig. 5. Despite the substantially smaller magnitude, these new distributions observed in Fig. 4 were unexpected, and they highlight the existence of a concurrent process of particle deposition during the mobilization of particles in the flushing stage 1. A phenomenon was previously hypothesized by Braga and Filion[19] through the direct observation of particle attachment at pipe wall samples which unexpectedly increased after flushing operations.

In addition, the mass flux curves from flushing stage 2 (Fig. 4) also revealed a second peak at one complete pipe loop turnover, which corresponds to the exit of the pipe loop length relative to the flushing direction. Such peaks suggest that additional particles were mobilized from the furthest upstream locations of the pipe loop, while the same positions were previously the furthest downstream locations for the opposite direction during flushing stage 1 (Fig. 3). Such locations, at the extremities of the pipe loop, match with wye-fittings that are used to route the water to the drain during flushing operations. In the forward direction, the water inlet occurs in the straight section of the upstream wye-fitting and its outlet occurs at the angle section of the downstream wye-fitting, these are reversed when the direction of the flow is reversed. For flushing in both directions, a length of approximately 0.5 m between the straight side of the downstream wye-fitting and its nearest valve forms a dead-end water volume at the end of the pipe loop. Given the increase of the mass flux rate that matches the wye-fitting position observed in the second flush stage (Fig. 4), it is hypothesized that in both the loading phase and in flushing stage 1, an additional accumulation of particles occurred in the downstream dead-ends formed by the wyes. Such material was further mobilized in the sequential flushing operation; this explains the peak that occurs at the full pipe loop volume turnover. This can be observed in the curves from experiments B and D in Fig. 3, which have a consistent distinct curvature around 1.0 pipe loop volume turnover; and in all curves from flushing stage 2 in Fig. 4, where particles from the previous flushing step were accumulated in its corresponding downstream wye-fittings. Dead ends have long been known as areas of poor water quality[12,13] and research has shown that dead end flushes are particularly effective at lowering turbidity and total iron.[18] The results of these experiments highlights that the passage of high concentrated particle suspensions around pipe fittings and intersections can also produce unexpected particle accumulation that can be diffused or advected to dead-end zones.

The redistribution of particles mobilized during unidirectional flushing could also have important implications for water utilities that use regular flushing to maintain water quality. Firstly, flushed pockets of accumulated material can be redistributed and contaminate other areas of a DWDS. This means that the amount of material mobilized during flushing is greater than the amount of material removed from the system. Loose particles that become mobilized during flushing may have the opportunity to become conditioned or more adhered to another downstream section of the pipes. Furthermore, inorganic particles are known to support biofilm growth,[26] and the deposition of these inorganic materials on pipe walls can aid in cell attachment and biofilm formation. Therefore, redistributed particles could encourage biofilm formation in other areas of the DWDS. The phenomenon of particle redistribution during unidirectional flushing could be an important reason why flushing operations typically only yield short term benefits in water quality.[5,18,22] New pipe sections could be susceptible to contamination from redistributed particles during flushing. Particles that are redistributed to new pipe sections could accelerate the material accumulation process in these sections. In other words, flushing may actually increase the material accumulation rate in new pipe sections and diminish long term water quality in those areas.

The mobilized mass of material from the flushing stages elucidates the effectiveness of reverse flushing as a method of mobilizing material from the pipe walls. Although small in comparison to F1, the amounts of mass mobilized in F2 and F4 are important because they represent particles that otherwise could not be mobilized by flushes in the previous direction. In other words, reversing the direction of flushing produces different phenomena than increasing the flow rate and shear stress and therefore the material being removed from one operation may be independent of the other. In addition, the material removed from the reverse direction flush was more adhered since the loose particles were likely removed in F1. In operational DWDS, the proportion of attached materials with higher MSS may be substantially higher than loose particulate materials. Therefore, it is important to develop strategies like a reverse direction flush that can remove adhered particles with high MSS.

Furthermore, the addition of biofilms could have large implications on the effectiveness of flushing in certain directions, because these living structures are highly adaptable to their environment and can develop a predominant resistance to the common flow direction.[27] Moreover, it is also hypothesized that particles can become embedded in biofilms, protecting them from shear forces at the pipe walls.[26–28] Thus, a flush in the opposite direction to the operational flow could have an outsized impact on material mobilization in pipes with biofilms.

Conclusions

A set of four experiments was conducted to evaluate the impact of reversing the flushing flow direction on the mobilization of iron oxide particles in a full-scale PVC pipe loop. Results showed that the first flushing operation was responsible for mobilizing most of the accumulated particles. However, during this operation, and under high wall shear stresses of 1.2 Pa, a small fraction of the resuspended particles was able to reattach to the pipe wall, forming new accumulation spots in previously clean pipe sections. A second flushing operation with the same magnitude but opposite flow direction triggered the mobilization of additional particles from the pipes. This finding points to the existence of under looked mechanisms of particle resistance to mobilization that are independent of the wall shear stresses. It is hypothesized that such mechanisms may arise from velocity profile transitions in system appurtenances that can create locations for enhanced particle accumulation. Further studies are required to verify the impact of both particle reattachment during flushing and enhanced accumulation on individual fittings in operational DWDSs. Overall, this work has helped improve our knowledge of the physical behaviour of accumulated particles in drinking water distribution systems and it can help water utilities improve flushing strategies to manage accumulated material in their systems.

Data availability

Data for this article, including information of flow rate, turbidity, suspended sediment concentration and particle size distribution measured during the experiments are available at **https://doi.org/10.5683/SP3/OOXTYZ**.

Conflicts of interest

There are no conflicts to declare.

Notes and references

1 V. Gauthier, B. Barbeau, R. Millette, J. Block and M. Prevost, Suspended particles in the drinking water of two distribution sytems, *Water Sci. Technol.: Water Supply*, 2001, **1**, 237–245.
2 A. Seth, R. Bachmann, J. B. Boxall, A. Saul and R. Edyvean, Characterisation of materials causing discolouration in potable water systems, *Water Sci. Technol.*, 2004, **49**, 27–32.
3 D. M. Cook and J. B. Boxall, Discoloration Material Accumulation in Water Distribution Systems, *J. Pipeline Syst. Eng. Pract.*, 2011, **2**, 113–122.
4 J. Vreeburg and J. B. Boxall, Discolouration in drinking water systems: a particular approach, *Water Res.*, 2007, **41**, 519–529.
5 A. Carrière, V. Gauthier, R. Desjardins and B. Barbeau, Evaluation of loose deposits in distribution systems through: unidirectional flushing, *J. AWWA*, 2005, **97**, 82–92.
6 P. S. Husband and J. B. Boxall, Asset deterioration and discolouration in water distribution systems, *Water Res.*, 2011, **45**, 113–124.
7 M. P. Ginige, J. Wylie and J. Plumb, Influence of biofilms on iron and manganese deposition in drinking water distribution systems, *Biofouling*, 2011, **27**, 151–163.
8 M. Farina, D. Silva Avila, J. Batista Teixeira da Rocha and M. Aschner, Metals, oxidative stress and neurodegeneration: a focus on iron, manganese and mercury, *Neurochem. Int.*, 2013, **62**, 575–594.
9 G. A. Wasserman, X. Liu, F. Parvez, H. Ahsan, D. Levy, P. Factor-Litvak, J. Kline, A. van Geen, V. Slavkovich, N. J. Lolacono, Z. Cheng, Y. Zheng and J. H. Graziano, Water manganese exposure and children's intellectual function in Araihazar, Bangladesh, *Environ. Health Perspect.*, 2006, **114**, 124–129.
10 Health Canada, *Manganese in drinking water*, 2016.
11 WHO, *Manganese in drinking water*, 2011.
12 E. N. Antoun, J. E. Dyksen and D. J. Hiltebrand, Unidirectional flushing: a powerful tool, *J. AWWA*, 1999, **91**, 62–72.
13 M. Friedman, G. J. Kirmeyer and E. Antoun, Developing and Implementing a Distribution System Flushing Program, *J. AWWA*, 2002, **94**, 48–56.
14 K. Oberoi, Distribution flushing program: the benefits and results, *AWWA Ann. Conf.*, New York, 1994.
15 J. H. Vreeburg, Discolouration in drinking water systems: a particular approach, *PhD Thesis*, Delft University of Technology, 2007.

16 E. Antoun, T. Tyson and D. Hiltebrand, Unidirectional flushing: A remedy to water quality problems such as biologically mediated corrosion, *AWWA Ann. Conf.*, Denver, 1997.
17 H. Armand, I. I. Stoianov and N. J. D. Graham, A holistic assessment of discolouration processes in water distribution networks, *Urban Water J.*, 2015, **14**, 263–277.
18 B. Barbeau, V. Gauthier, K. Julienne and A. Carriere, Dead-end flushing of a distribution system: Short and long-term effects on water quality, *J. Water Supply:Res. Technol.–AQUA*, 2005, **54**, 371–383.
19 A. Braga and Y. Filion, Initial stages of particulate iron oxide attachment on drinking water PVC pipes characterized by turbidity data and brightfield microscopy from a full-scale laboratory, *Environ. Sci.: Water Res. Technol.*, 2022, **8**, 1195–1210.
20 A. S. Braga and Y. Filion, The interplay of suspended sediment concentration, particle size and fluid velocity on the rapid deposition of suspended iron oxide particles in PVC drinking water pipes, *Water Res.:X*, 2022, **15**, 100–143.
21 A. S. Benson, A. M. Dietrich and D. L. Gallagher, Evaluation of Iron Release Models for Water Distribution Systems, *Crit. Rev. Environ. Sci. Technol.*, 2012, **42**, 44–97.
22 J. B. Boxall, M. Blokker, P. Schaap, V. Speight and S. Husband, Managing discolouration in drinking water distribution systems by integrating understanding of material behaviour, *Water Res.*, 2023, **243**, 120–416.
23 H.-C. Flemming, J. Wingender, U. Szewzyk, P. Steinberg, S. A. Rice and S. Kjelleberg, Biofilms: an emergent form of bacterial life, *Nat. Rev. Microbiol.*, 2016, **14**, 563–575.
24 J. B. Boxall, A. J. Saul, J. D. Gunstead and N. Dewis, Regeneration of discolouration in distribution systems, *World Water & Environmental Resources Congress*, 2003, pp. 1–9.
25 J. B. Boxall and A. J. Saul, Modeling discolouration in potable water distribution systems, *J. Environ. Eng.*, 2005, **55**, 207–219.
26 I. Douterelo, R. Sharpe and J. Boxall, Bacterial community dynamics during the early stages of biofilm formation in a chlorinated experimental drinking water distribution system: implications for drinking water discolouration, *J. Appl. Microbiol.*, 2014, **117**, 286–301.
27 K. E. Fish, R. Collins, N. H. Green, R. L. Sharpe, I. Douterelo and M. A. Osborn, *et al.*, Characterisation of the physical composition and microbial community structure of biofilms within a model full-scale drinking water distribution system, *PLoS One*, 2015, **10**(2), e0115824.
28 K. Fish, A. M. Osborn and J. B. Boxall, Biofilm structures (EPS and bacterial communities) in drinking water distribution systems are conditioned by hydraulics and influence discolouration, *Sci. Total Environ.*, 2017, 571–580.

